TECHNICAL REPORT RG-7T-6

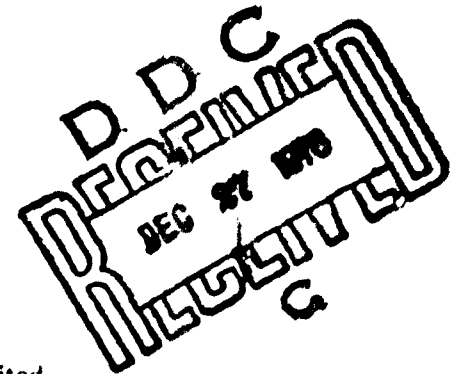# FREQUENCY DOMAIN IDENTIFICATION
OF GYRO DRIFT COEFFICIENTS

R. E. Pugh
Guidance and Control Directorate
US Army Missile Research, Development and Engineering Laboratory
US Army Missile Command
Redstone Arsenal, Alabama 35809

and

J. C. Hung
The University of Tennessee
Knoxville, Tennessee

30 August 1976

U.S. ARMY MISSILE COMMAND
Redstone Arsenal, Alabama 35809

DISPOSITION INSTRUCTIONS

DISCLAIMER

TRADE NAMES

REPORT DOCUMENTATION PAGE		READ INSTRUCTIONS BEFORE COMPLETING FORM
1. REPORT NUMBER RG-7T-6	2. GOVT ACCESSION NO.	3. RECIPIENT'S CATALOG NUMBER
4. TITLE *(and Subtitle)* FREQUENCY DOMAIN IDENTIFICATION OF GYRO DRIFT COEFFICIENTS .		5. TYPE OF REPORT & PERIOD COVERED Technical Report.
		6. PERFORMING ORG. REPORT NUMBER RG-7T-6
7. AUTHOR(s) R. E. Pugh MICOM J. C. Hung University of Tennessee		8. CONTRACT OR GRANT NUMBER(s)
9. PERFORMING ORGANIZATION NAME AND ADDRESS Commander US Army Missile Command ATTN: DRSMI-RG Redstone Arsenal, Alabama 35809		10. PROGRAM ELEMENT, PROJECT, TASK AREA & WORK UNIT NUMBERS DA Project 1X364307D212 AMCMS Code 634307.12.17100
11. CONTROLLING OFFICE NAME AND ADDRESS Commander US Army Missile Command ATTN: DRSMI-RPR Redstone Arsenal, Alabama 35809		12. REPORT DATE 30 August 1976
		13. NUMBER OF PAGES 28
14. MONITORING AGENCY NAME & ADDRESS *(If different from Controlling Office)*		15. SECURITY CLASS. *(of this report)* UNCLASSIFIED
		15a. DECLASSIFICATION/DOWNGRADING SCHEDULE

16. DISTRIBUTION STATEMENT *(of this Report)*

Approved for public release; distribution unlimited.

17. DISTRIBUTION STATEMENT *(of the abstract entered in Block 20, if different from Report)*

18. SUPPLEMENTARY NOTES

19. KEY WORDS *(Continue on reverse side if necessary and identify by block number)*

Two-axis tumble test
Frequency domain data reduction
Data processing algorithm
Gyro drift parameters

20. ABSTRACT *(Continue on reverse side if necessary and identify by block number)*

This report presents a new two-axis tumble test for the determination of gyro drift parameters. The method uses the concept of frequency domain data reduction which helps to lessen the required test procedure and the needed test equipment. Both the test procedure and data processing algorithm are presented in detail. The result of a simulated testing is included to demonstrate the proposed concept.
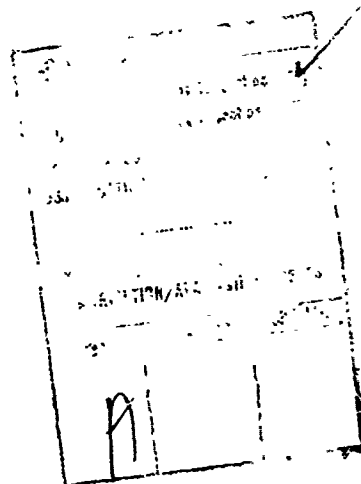
DD FORM 1473 1 JAN 73 EDITION OF 1 NOV 65 IS OBSOLETE

CONTENTS

Page

1

I.   INTRODUCTION

The use of precision inertial sensors for high performance applications demands accurate identification of drift coefficients. This identification technique consists of two parts: testing and data reduction. An acceptable identification technique should be low cost.

There are at least three different objectives for testing. First, development tests are conducted in laboratories for verifying concepts, gaining intuitions, exploring desired modifications, and searching for proper parameter values. Second, acceptance tests are used by manufacturers and customers to determine if the specifications are met. Third, calibration tests are used to determine sensor parameters.

This report concerns test and data reduction techniques for single-degree-of-freedom gyros. Techniques for two-degree-of-freedom gyros are similar in concept and therefore will not be discussed in this report.

The most important aspects of gyro testing for navigation and guidance purposes are those concerned with drift errors. There are at least four different types of testing methods for the determination of drift parameters [1, 2, 3, 4, 5, and 6]. They are as follows:

a)   Six position rate test.

b)   Six position static test.

c)   Single-axis tumble test.

d)   Two-axis tumble test.

All methods require the use of a test table. Both the six position rate and static tests are time consuming, because they require repeated reorientation of the gyro and a long settling time after each reorientation. The single-axis tumble test does not generate sufficient information for the determination of drift parameters of a high precision drift model. Among the four methods, the two-axis tumble test is the latest technique. Compared to the others, it has several advantages which will be discussed in a later section. However, the known two-axis tumble test requires the knowledge of the attitude of the gyro case at every data taking instant.

This report presents a new two-axis tumble test and data reduction technique. The method uses a new concept for obtaining all drift parameters from the measurement record. The concept does not need the knowledge of the gyro case attitude at each data taking instant. Thus, much simpler test equipment can be used. The report will first review the development of an analytic model for drift parameters. The test procedure for the proposed new two-axis tumble test will be described, followed by the development of the data processing algorithm. A comparison between the old and new methods will be made. The result

3
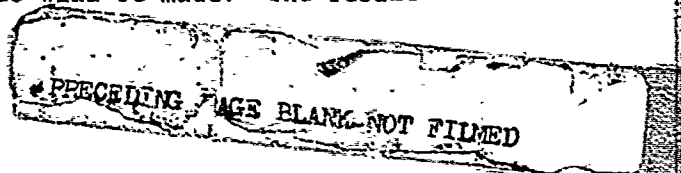
of a simulation using the proposed technique will be included and dis-
cussed. For the convenience of the reader, a list of references and
an appendix are attached.

II. ANALYTIC MODEL FOR GYRO DRIFT

Gyro drifts may be classified into three types: constant
drifts, acceleration sensitive drifts, and drifts which are sensitive
to the products of accelerations [7].

The constant drifts are caused by the spring force of flex leads
and by the electrical reaction torques excited on the gimbal. All
constant drifts will be lumped together and represented by D_o.

Most of the acceleration sensitive drifts are caused by mass
unbalance of the gimbal-rotor assembly. This unbalance of mass results
in a displacement between the gimbal output axis and the mass center
of the gimbal-rotor assembly. This displacement is denoted by $\underline{d}$ which
is a vector in the three-dimensional space. Let $\hat{s}$, $\hat{i}$, and $\hat{o}$ be three
unit vectors pointed along the spin reference axis, input axis, and
output axis of the gyro, respectively. Let $\underline{a}$ be the acceleration
vector of the gyro case and m be the mass of the gimbal-rotor assembly.
The inertial torque about the output axis due to the acceleration is
given by

$$T_m = -m(\underline{d} \times \underline{a}) \cdot \hat{o} = m(d_i a_s - d_s a_i)$$

where "×" and "·" denote cross-product and dot-product, respectively.
The subscripts s and i are used to denote those vector components which
are in the directions of $\hat{s}$ and $\hat{i}$, respectively. Because drift is
linearly proportional to torque, the mass unbalance drift may be repre-
sented by

$$D_m = K_s\, a_s + K_i\, a_i \tag{1}$$

where K_s and K_i are proportionality constants.

Another source of acceleration sensitive drift is the thermo-
convection torque for a gyro with floated gimbal. When the mass is not
balanced, the thermo-convection in the fluid generates a torque along
the output axis. This torque is proportional to the mass m, off-center
displacement d_o, and the acceleration component a_o, where subscript o
denotes the vector components in the direction of $\hat{o}$. The corresponding
drift may be represented by

4

$$D_{th} = K_o a_o \qquad (2)$$

where k_o is a proportional constant. It is noted that D_{th} is due to the combined effect of mass unbalance, thermo-convection of the fluid, and the acceleration of gyro case along the $\hat{o}$ direction.

The drifts which are sensitive to the product of accelerations are caused by the deflection of the gimbal assembly under acceleration. The phenomena is often referred to as anisoelastic effect. The relationship between the deflection and acceleration can be expressed as

$$\underline{\Delta} = mC\underline{a}$$

where $\underline{\Delta}$ is the deflection vector and C is a 3×3 compliance matrix given by

$$C = \begin{bmatrix} c_{ss} & c_{si} & c_{so} \\ c_{is} & c_{ii} & c_{io} \\ c_{os} & c_{oi} & c_{oo} \end{bmatrix} .$$

For each double-subscripted element of C, the first subscript denotes the direction of deflection and the second the direction of acceleration. The deflection $\underline{\Delta}$ causes a mass unbalance. Together, they generate a torque about the output axis given by

$$T_c = -m(\underline{\Delta} \times \underline{a}) \cdot \hat{o} = \left\{ m^2 (c_{ss} - c_{ii}) a_s a_i + c_{so} a_i a_o \right.$$
$$\left. + c_{si} a_i^2 - c_{is} Q_s^2 - c_{io} a_o a_s \right\} .$$

Each of the terms in this equation can produce a nonzero average torque in the presence of vibrations of the same frequency. The gyro drift caused by torque T_c may be represented by

$$D_K = K_{ss} a_s^2 + K_{ii} a_i^2 + K_{si} a_s a_i + K_{io} a_i a_o + K_{os} a_o a_s . \qquad (3)$$

Adding Equations (1), (2), (3), and D_o gives the desired analytic model of the total drift for the gyro:

$$D = D_o + K_s a_s + K_i a_i + K_o a_o + K_{ss} a_s^2 + K_{ii} a_i^2 + K_{si} a_s a_i$$

$$+ K_{io} a_i a_o + K_{os} a_o a_s \quad . \tag{4}$$

Equation (4) shows that the total drift D consists of nine terms, characterized by drift parameters D_o and K's. Because a different type of compensation is required for a different type of drift, identification of these parameters is essential.

III. A NEW TWO-AXIS TUMBLE TEST

Identification of the nine drift parameters by testing requires that all nine drift modes as shown in Equation (4) be excited by test signals. This can be accomplished by tumbling the gyro about two orthogonal axes. The proposed two-axis tumble test consists of two parts: performance of the experiment and data processing for drift parameter identification. These two parts are interrelated, because the required measurements depend on the way data are processed.

Figure 1 shows a gyro test stand. The stand has two rotatable axes which are perpendicular to each other. The gyro under test is mounted on the second turntable with its input axis (IA) precisely aligned to the table axis; therefore, the gyro can be made to tumble about two axes. In Figure 1, SRA and OA indicate direction of spin reference axis and output axis, respectively.

The test is performed with the table axis positioned parallel to the earth rotational axis. The first table axis is elevated to the local latitude angle λ from the horizontal plane. Under this condition, IA is perpendicular to polar axis and the gyro will not sense the earth rate.

Let the first table be rotated at an angular rate ω_ϕ and the second table be rotated about the IA axis at an angular rate ω_θ. The gyro senses ω_θ but not ω_ϕ. Let ω_R be the gyro output. Because ω_θ is known, the difference between ω_R and ω_θ, which is the total drift, can be calculated. In equation form,

$$D = \omega_R - \omega_\theta \quad . \tag{5}$$

To avoid the earth rate effect which may be caused by imperfect alignment of the table axis to the polar axis, it is desirable to turn the table at a rate approximately ten to twenty times faster than the earth
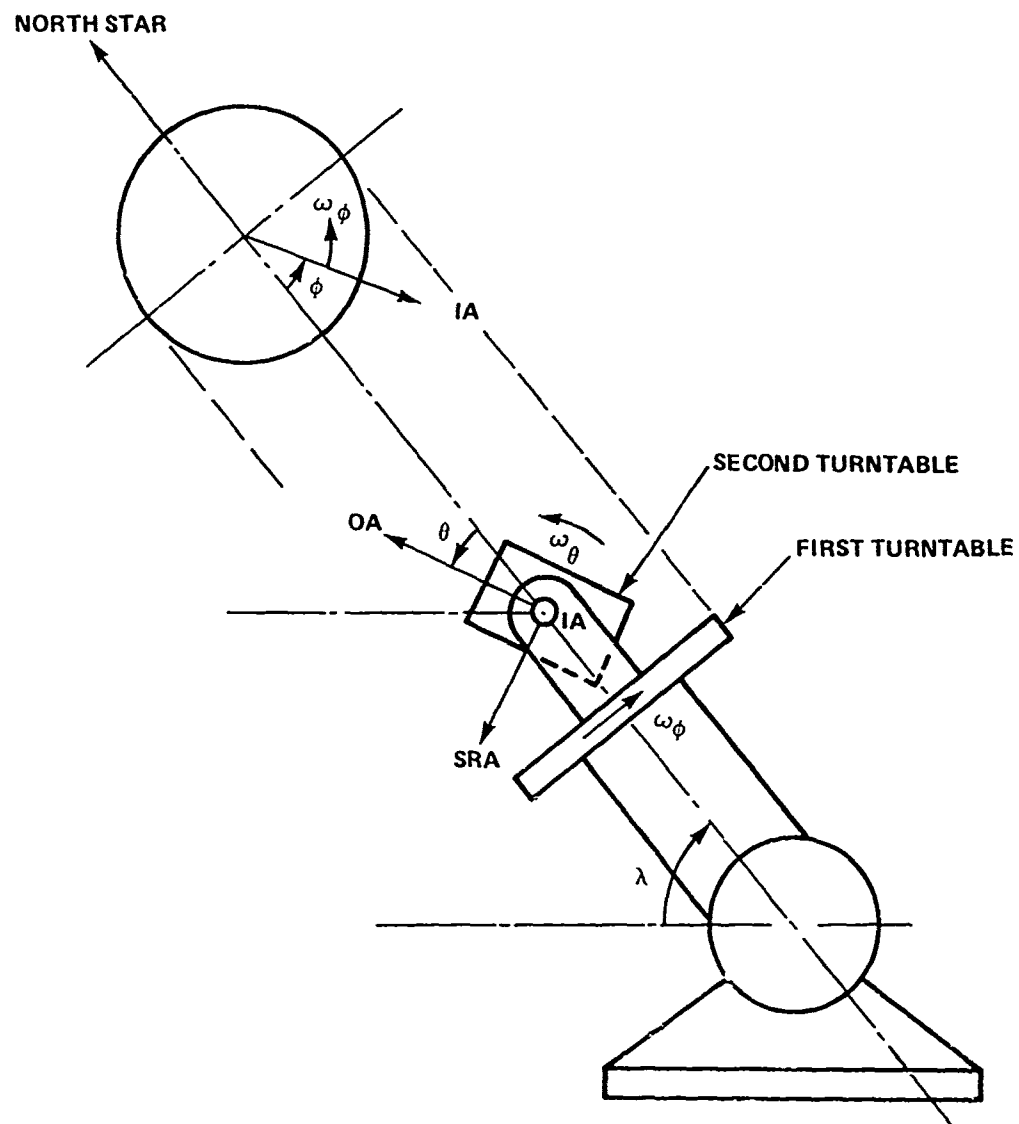
6

Figure 1. Gyro test stand.

rate. To have a good frequency separation property for the drift
signal, which will be discussed later, the rotation rate of the second
axis should be approximately five times that of the table axis. A
reasonable data taking interval is every $6°$ to $12°$ of the second axis
rotation. More data points allow a better statistical data reduction.
The required data record covers a full rotation of the first axis, or
one of its integer multiples.

The remaining problem is the determination of nine drift parameters
from the measured values of D by means of computer data processing.

IV.   DATA PROCESSING ALGORITHM

A.   The Measurement Equation

Equation (4) shows that eight of the nine drift terms are
dependent on either components of acceleration or on their products.
Because the test stand is stationary, the acceleration components experi-
enced by the gyro are due to earth gravitation. The value of each accel-
eration component, in turn, depends on the angular positions of the first
and second table axes. These angular positions are represented by
ϕ and θ as shown in Figure 1 where their references of measurement are
also indicated.

The acceleration components experienced by the gyro can be obtained
with the help of Figure 2. The accelerations along the spin reference
axis, input axis, and output axis are given, respectively, by

$$a_s = g \cos \lambda \cos \theta \cos \phi + g \sin \lambda \sin \theta \tag{6}$$

$$a_i = -g \cos \lambda \sin \phi \tag{7}$$

$$a_o = g \cos \lambda \cos \phi \sin \theta - g \sin \lambda \cos \theta \tag{8}$$

where g is the earth gravitation. Let

$$\theta = \omega_\theta t \tag{9}$$

$$\phi = \omega_\phi t \quad . \tag{10}$$

8

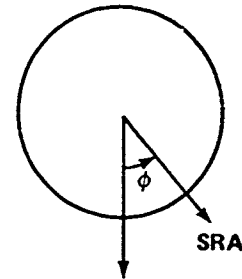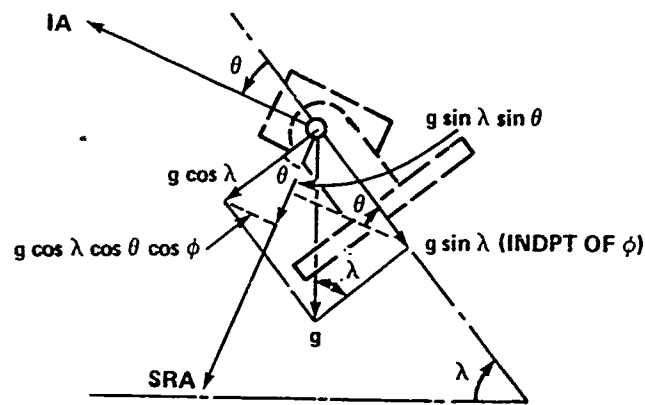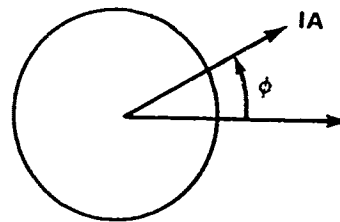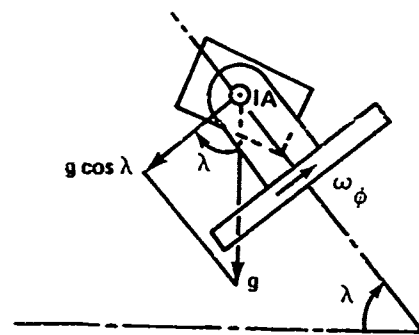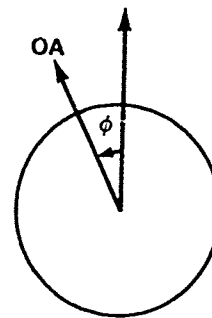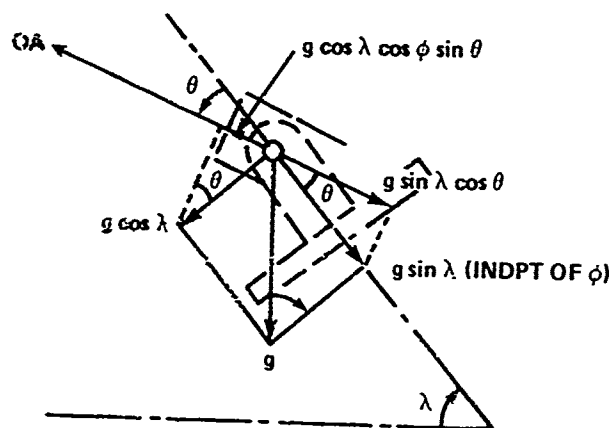(a) $A_S = g \cos \lambda \cos \theta \cos \phi + g \sin \lambda \sin \theta$

(b) $A_I = -g \cos \lambda \sin \phi$

(c) $A_O = g \cos \lambda \cos \phi \sin \theta - g \sin \lambda \cos \theta$

Figure 2. Acceleration components.

Then Equations (6), (7), and (8) become

$$a_s = g \cos \lambda \cos \omega_\theta t \cos \omega_\phi t + g \sin \lambda \sin \omega_\theta t \qquad (11)$$

$$a_i = -g \cos \lambda \sin \omega_\phi t \qquad (12)$$

$$a_o = g \cos \lambda \cos \omega_\phi t \sin \omega_\theta t - g \sin \lambda \cos \omega_\theta t \quad . \qquad (13)$$

Substituting the three preceding equations into Equation (4) gives the total drift as a function of time t; or, equivalently as a function of the angular positions of the table and the gyro house. The explicit form of the total drift is

$$D = D_o + K_s \{g \cos \lambda \cos \omega_\theta t \cos \omega_\phi t + g \sin \lambda \sin \omega_\theta t\}$$

$$- K_i \{g \cos \lambda \sin \omega_\phi t\}$$

$$+ K_o \{g \cos \lambda \cos \omega_\phi t \sin \omega_\theta t - g \sin \lambda \cos \omega_\theta t\}$$

$$+ K_{ss} \{g \cos \lambda \cos \omega_\theta t \cos \omega_\phi t + g \sin \lambda \sin \omega_\theta t\}^2$$

$$+ K_{ii} \{g \cos \lambda \sin \omega_\phi t\}^2$$

$$- K_{si} \{g \cos \lambda \cos \omega_\theta t \cos \omega_\phi t + g \sin \lambda \sin \omega_\theta t\} \times \{g \cos \lambda \sin \omega_\phi t\}$$

$$- K_{io} \{g \cos \lambda \sin \omega_\phi t\} \times \{g \cos \lambda \cos \omega_\phi t \sin \omega_\theta t - g \sin \lambda \cos \omega_\theta t\}$$

$$- K_{os} \{g \sin \lambda \cos \omega_\theta t - g \cos \lambda \cos \omega_\phi t \sin \omega_\theta t\}$$

$$\times \{g \cos \lambda \cos \omega_\theta t \cos \omega_\phi t + g \sin \lambda \sin \omega_\theta t\} \quad . \qquad (14)$$

Equation (14) contains terms which are products of two frequencies, indicating the existance of modulation process. As a result, extra frequency components are generated. With the aid of trigonometric identities, Equation (14) can be rearranged as a sum of several groups; each is associated with one frequency as follows:

10

$$D = \left[D_o + K_{ss}\left(\frac{D_1}{2} + D_2\right) + K_{ii}D_1\right] - [K_I D_4 \sin \omega_\phi t]$$

$$+ \left[\left(K_{ss}\frac{D_1}{2} - K_{ii}D_1\right)\cos 2\omega_\phi t\right]$$

$$+ \left[K_{si}\frac{D_1}{2}\sin(\omega_\theta - 2\omega_\phi)t - K_{io}\frac{D_1}{2}\cos(\omega_\theta - 2\omega_\phi)t\right]$$

$$+ \left[\left(K_s\frac{D_4}{2} - K_{si}\frac{D_3}{2}\right)\cos(\omega_\theta - \omega_\phi)t + \left(K_o\frac{D_4}{2} - K_{io}\frac{D_3}{2}\right)\sin(\omega_\theta - \omega_\phi)t\right]$$

$$+ [K_s D_5 \sin \omega_\theta t - K_o D_5 \cos \omega_\theta t]$$

$$+ \left[\left(K_s\frac{D_4}{2} + K_{si}\frac{D_3}{2}\right)\cos(\omega_\theta + \omega_\phi)t + \left(K_o\frac{D_4}{2} + K_{io}\frac{D_3}{2}\right)\sin(\omega_\theta + \omega_\phi)t\right]$$

$$+ \left[K_{io}\frac{D_1}{2}\cos(\omega_\theta + 2\omega_\phi)t - K_{si}\frac{D_1}{2}\sin(\omega_\theta + 2\omega_\phi)t\right]$$

$$+ \left[K_{ss}\frac{D_1}{4}\cos 2(\omega_\theta - \omega)t + K_{os}\frac{D_1}{4}\sin 2(\omega_\theta - \omega_\phi)t\right]$$

$$+ \left[K_{ss}\frac{D_3}{2}\sin(2\omega_\theta - \omega_\phi)t - K_{os}\frac{D_3}{2}\cos(2\omega_\theta - \omega_\phi)t\right]$$

$$+ \left[K_{ss}\left(\frac{D_1}{2} - D_2\right)\cos 2\omega_\theta t + K_{os}\left(\frac{D_1}{2} - D_2\right)\sin 2\omega_\theta t\right]$$

$$+ \left[K_{ss}\frac{D_3}{2}\sin(2\omega_\theta + \omega_\phi)t - K_{os}\frac{D_3}{2}\cos(2\omega_\theta + \omega_\phi)t\right]$$

$$+ \left[K_{os}\frac{D_1}{4}\sin 2(\omega_\theta + \omega_\phi)t + K_{ss}\frac{D_1}{4}\cos 2(\omega_\theta + \omega_\phi)t\right] \qquad (15)$$

where

$$\left.\begin{aligned}
D_1 &= \frac{g^2 \cos^2 \lambda}{2}\\[6pt]
D_2 &= \frac{g^2 \sin^2 \lambda}{2}\\[6pt]
D_3 &= \frac{g^2 \sin 2\lambda}{2}\\[6pt]
D_4 &= g \cos \lambda\\[6pt]
D_5 &= g \sin \lambda
\end{aligned}\right\} \qquad (16)$$

11

Equation (15) is the measurement equation sought. The equation relates the total drift D to drift parameters which are D_o and K's. It is noted that the total drift contains thirteen different frequency components. The right-hand side of the equation is arranged into thirteen terms; each term gives one frequency component.

B. Use of Fourier Analysis

If values of ω_ϕ and ω_θ are property chosen, the thirteen frequencies in the drift signal can be distinctly separated from each other. Then the amplitudes and phases of respective frequency components can be determined from the measured drift signal by performing a Fourier analysis of the signal. This can be effected by using either a Fast Fourier transformation (FFT) or by Fourier coefficient determination [8]. In terms of amplitudes and phases, Equation (15) has the form

$$D = A_1 + A_2 \sin(\omega_\phi t + \beta_2) + A_3$$

$$+ A_4 \sin[(\omega_\theta - 2\omega_\phi)t + \beta_4] + A_5 \sin[(\omega_\theta - \omega_\phi)t + \beta_5]$$

$$+ A_6 \sin(\omega_\theta t + \beta_6) + A_7 \sin[(\omega_\theta + \omega_\phi)t + \beta_7]$$

$$+ A_8 \sin[(\omega_\theta + 2\omega_\phi)t + \beta_8] + A_9 \sin[2(\omega_\theta - \omega_\phi)t + \beta_9]$$

$$+ A_{10} \sin[(2\omega_\theta - \omega_\phi)t + \beta_{10}] + A_{11} \sin(2\omega_\theta t + \beta_{11})$$

$$+ A_{12} \sin[(2\omega_\theta + \omega_\phi) + \beta_{12}] + A_{13} \sin[2(\omega_\theta + \omega_\phi)t + \beta_{13}] \qquad (17)$$

where

$$A_1 = D_o + K_{ss}\left(\frac{D_1}{2} + D_2\right) + K_{ii}D_1 \qquad (18)$$

$$A_2 = K_i D_4 \qquad (19)$$

$$A_3 = K_{ss}\frac{D_1}{2} - K_{ii}D_1 \qquad (20)$$

$$A_4 = \sqrt{\left(K_{si}\frac{D_1}{2}\right)^2 + \left(K_{io}\frac{D_1}{2}\right)^2} \qquad (21)$$

12

$$A_5 = \sqrt{\left(K_s \frac{D_4}{2} - K_{si} \frac{D_3}{2}\right)^2 + \left(K_o \frac{D_4}{2} - K_{io} \frac{D_3}{2}\right)^2} \tag{22}$$

$$A_6 = \sqrt{(K_s D_5)^2 + (K_o D_5)^2} \tag{23}$$

$$A_7 = \sqrt{\left(K_s \frac{D_4}{2} + K_{si} \frac{D_3}{2}\right)^2 + K_o\left(\frac{D_4}{2} + K_{io} \frac{D_3}{2}\right)^2} \tag{24}$$

$$A_8 = A_4 \tag{25}$$

$$A_9 = \sqrt{\left(K_{ss} \frac{D_1}{4}\right)^2 + \left(K_{os} \frac{D_1}{4}\right)^2} \tag{26}$$

$$A_{10} = \sqrt{\left(K_{ss} \frac{D_3}{2}\right)^2 + \left(K_{os} \frac{D_3}{2}\right)^2} \tag{27}$$

$$A_{11} = \sqrt{K_{ss}^2 \left(\frac{D_1}{2} - D_2\right)^2 + K_{os}^2 \left(\frac{D_1}{2} - D_2\right)^2} \tag{28}$$

$$A_{12} = A_{10} \tag{29}$$

$$A_{13} = A_9 \tag{30}$$

and

$$\beta_1 = 0 \tag{31}$$

$$\beta_2 = 180 \tag{32}$$

$$\beta_3 = 90° \tag{33}$$

$$\beta_4 = \tan^{-1}\left(\frac{-K_{io}}{K_{si}}\right) \quad (4\text{th } q_1) \tag{34}$$

$$\beta_5 = \tan^{-1} \frac{K_s D_4 - K_{si} D_3}{K_o D_4 - K_{io} D_3} \quad (1\text{st } q_1) \tag{35}$$

13

$$\beta_6 = \tan^{-1}\left(\frac{K_o}{K_s}\right) \qquad \text{(4th } q_1\text{)} \tag{36}$$

$$\beta_7 = \tan^{-1}\frac{K_s D_4 + K_{si} D_3}{K_o D_4 + K_{io} D_3} \qquad \text{(1st } q_1\text{)} \tag{37}$$

$$\beta_8 = \tan^{-1}\left(\frac{-K_{io}}{K_{si}}\right) \qquad \text{(2nd } q_1\text{)} \tag{38}$$

$$\beta_9 = \tan^{-1}\left(\frac{K_{ss}}{K_{os}}\right) \qquad \text{(1st } q_1\text{)} \tag{39}$$

$$\beta_{10} = \tan^{-1}\left(\frac{-K_{os}}{K_{ss}}\right) \qquad \text{(4th } q_1\text{)} \tag{40}$$

$$\beta_{11} = \tan^{-1}\left(\frac{K_{ss}}{K_{os}}\right) \qquad \text{(1st } q_1\text{)} \tag{41}$$

$$\beta_{12} = \tan^{-1}\left(\frac{-K_{os}}{K_{ss}}\right) \qquad \text{(4th } q_1\text{)} \tag{4-}$$

$$\beta_{13} = \tan^{-1}\left(\frac{K_{ss}}{K_{os}}\right) \qquad \text{(1st } q_1\text{)} \quad . \qquad . \tag{43}$$

The parentheses following each angle indicate the quadrant of the angle.

Equations (18) to (43) consist of a total of twenty-six equations. They are used to solve for the nine drift coefficients after A_i and B_i, $i = 1, \ldots, 13$, are determined from the Fourier analysis of the drift signal. There are more equations than unknowns, indicating redundant information. Maximum use of the information will minimize the effect of instrument noise on the determination of drift coefficients from the Fourier coefficients. The method chosen for reducing the redundant information to an unique set of drift coefficients is the well-known least square regression [9, 10].

C. Use of Least Square Regression

Squaring both sides of Equations (26) to (30), combining the result with Equations (39) to (43), and arranging these ten equations in a matrix equation form, gives

14

$$
\begin{bmatrix}
\left(\dfrac{4\,A_9}{D_1}\right)^2 \\[12pt]
\left(\dfrac{2\,A_{10}}{D_3}\right)^2 \\[12pt]
\left(\dfrac{2\,A_{11}}{D_1 + 2D_2}\right)^2 \\[12pt]
\left(\dfrac{2\,A_{12}}{D_3}\right)^2 \\[12pt]
\left(\dfrac{4\,A_{13}}{D_1}\right)^2 \\[12pt]
0 \\[6pt]
0 \\[6pt]
0 \\[6pt]
0 \\[6pt]
0
\end{bmatrix}
=
\begin{bmatrix}
1 & 1 \\
1 & 1 \\
1 & 1 \\
1 & 1 \\
1 & 1 \\
1 & -\tan^2\beta_9 \\
1 & -\cot^2\beta_{10} \\
1 & -\tan^2\beta_{11} \\
1 & -\cot^2\beta_{12} \\
1 & -\tan^2\beta_{13}
\end{bmatrix}
\begin{bmatrix}
K_{ss}^2 \\[12pt]
K_{os}^2
\end{bmatrix}
\qquad (44)
$$

$$\underbrace{}_{\underline{u}} \qquad \underbrace{}_{M}$$

Vector $\underline{u}$ and matrix M are defined as shown in Equation (44). A well-known least square regression formula gives [9]

$$
\begin{bmatrix}
K_{ss}^2 \\[12pt]
K_{os}^2
\end{bmatrix}
= (M^T M)^{-1} M^T \underline{u} \qquad . \qquad (45)
$$

By taking the square root of Equation (45) and retaining the positive values, K_{ss} and K_{os} are determined.

Similarly, squaring, summing, and rearranging, Equations (21) to (25) and (34) to (38) can give

15

$$
\underbrace{\begin{bmatrix} \left(\dfrac{A_6}{D_5}\right)^2 \\[2mm] \left(\dfrac{2\,A_4}{D_1}\right)^2 \\[2mm] \left(\dfrac{2\,A_8}{D_1}\right)^2 \\[2mm] 2(A_5^2 + A_7^2) \\[2mm] 0 \\[2mm] 0 \\[2mm] 0 \\[2mm] 0 \end{bmatrix}}_{\underline{v}}
=
\underbrace{\begin{bmatrix} 1 & 1 & 0 & 0 \\[2mm] 0 & 0 & 1 & 1 \\[2mm] 0 & 0 & 1 & 1 \\[2mm] D_4^2 & D_4^2 & D_3^2 & D_3^2 \\[2mm] 1 & -\cot^2 \beta_6 & 0 & 0 \\[2mm] 0 & 0 & -\tan^2 \beta_4 & 1 \\[2mm] 0 & 0 & -\tan^2 \beta_8 & 1 \\[2mm] D_4^2 & -aD_4^2 & -D_3^2 & aD_3^2 \end{bmatrix}}_{N}
\begin{bmatrix} K_s^2 \\[2mm] K_o^2 \\[2mm] K_{si}^2 \\[2mm] K_{io}^2 \end{bmatrix}
\qquad (46)
$$

where

$$
a = \tan \beta_5 \, \tan \beta_7 \quad . \tag{47}
$$

Vector $\underline{v}$ and matrix N are defined as shown in Equation (46); the least square solution for the equation is

$$
\begin{bmatrix} K_s^2 \\[2mm] K_o^2 \\[2mm] K_{si}^2 \\[2mm] K_{io}^2 \end{bmatrix}
= (N^T N)^{-1} N^T \underline{v} \quad . \tag{48}
$$

16

Taking the positive values of the square root of Equation (48) gives K_s, K_o, K_{si}, and K_{io}.

Finally, using Equations (20), (19), and (18) in this order, the following formulas are obtained:

$$K_{ii} = \frac{K_{ss}}{2} - \frac{A_3}{D_1} \tag{49}$$

$$K_i = \frac{A_2}{D_4} \tag{50}$$

$$D_o = A_1 - K_{ss}\left(\frac{D_1}{2} + D_2\right) - K_{ii}D_1 \quad . \tag{51}$$

Thus, all nine drift parameters are determined.

D. Discussion

A striking difference between the new and the old two-axis tumble tests is that the former does not require the knowledge of the time instant at each data point (or equivalently, the attitude of the second axis at each data point). This allows the use of simpler test equipment and demands less operator effort. The conceptual difference is that in the new method the drift parameter identification is performed using the frequency domain information while in the latter method identification is done using the time domain information. It should be mentioned that the new method reduces the operator's effort and lessens the test equipment requirement at the expense of a slightly more complex data processing algorithm. Because both the new and the old method require a computer for data processing and because the computer time required for either method is insignificant, the trade-off favors the new method.

On the other hand, both the new and old two-axis tumble tests have the following advantages as compared to the other three methods listed in the Introduction. First, there is no need of repeated gyro repositioning which is time-consuming. Second, because both the first and second tables are turning at constant speed, there is no motion-induced transient effect in the measured drift signal. Third, the measured drift signal provides sufficient information for the determination of all nine, rather than partial, drift parameters. Fourth, the required test time is shorter.

Finally, to be truly objective, it should be mentioned that the old two-axis tumble test has one advantage over the new method. When using the old method, the required data record can be of any length as long as it contains at least nine data points. In other words, the test operator

does not have to wait for the table to turn a full revolution although the reduced data record may not provide sufficient redundancy for a good statistical data processing. The algorithm for the old method is included as the Appendix for the reader's reference.

V. SIMULATION RESULT

Simulated testing was conducted to demonstrate the proposed method. The simulation was performed with the first table turning about its axis at twenty times the earth rate and the second table turning about its axis at 100 times the earth rate. The gyro drift was simulated. For a full rotation of the table, 864 data points were generated.

With the chosen rotation rates for the two tables, the generated frequency components in the drift signal are evenly separated by a frequency separation of 20 Hz. Table 1 lists all the frequency components. The amplitudes and tangent of the phases of the frequency components as generated by Fourier analysis are shown in Table 2. All nine drift coefficients resulting from the least square regression are shown in Table 3. The effectiveness of the identification technique and the correctness of the data reduction algorithm are demonstrated. The discrepancies are evidently due to computation errors, which can be reduced by using the double precision computation. However, the identification accuracy as shown in Table 3 is sufficient for most applications.

VI. CONCLUSION

A frequency domain technique for the identification of gyro drift coefficients has been developed. The technique involves a two-axis tumble test and an unique data reduction. Compared to other techniques, this technique has the merit of providing more complete data for describing gyro drift characteristics. In addition, the required procedure for testing and data reduction can be conveniently implemented into an automated gyro drift coefficient identification system.

A simulation was performed. The result demonstrated the effectiveness of the gyro drift coefficient determination technique and the correctness of the data reduction algorithm.

TABLE 1. FREQUENCY COMPONENTS IN DRIFT SIGNAL

Frequency Component	Frequency Value (Hz)
d-c	0
ω_ϕ	20
$2\omega_\phi$	40
$\omega_\theta - \omega_\phi$	60
$\omega_\theta - \omega_\phi$	80
ω_θ	100
$\omega_\theta + \omega_\phi$	120
$\omega_\theta + 2\omega_\phi$	140
$2(\omega_\theta - \omega_\phi)$	160
$2\omega_\theta - \omega_\phi$	180
$2\omega_\theta$	200
$2\omega_\theta + \omega_\phi$	220
$2(\omega_\theta + \omega_\phi)$	240

TABLE 2. RESULT OF FOURIER ANALYSIS

Frequency	Real Part	Imaginary Part
dc	0.82279050	---
20	-0.00000126	-0.22565949
40	0.00138369	-0.00000834
60	-0.00023610	0.00023035
80	0.08428782	0.01377910
100	-0.01948988	0.11692071
120	0.08493614	0.01442608
140	0.00023283	-0.00023330
160	0.00023244	0.00011725
180	-0.00032030	0.00064254
200	0.00002115	0.00001165
220	-0.00032045	0.00064246
240	0.00023199	0.00011721

TABLE 3. IDENTIFIED DRIFT COEFFICIENTS

Drift Coefficient	Value		Discrepancy (%)
	Identified	Actual	
D_o (deg/hr)	5.999820	6.0	0.003
K_s (deg/hr/g)	2.999528	3.0	0.016
K_i (deg/hr/g)	4.000009	4.0	0.0002
K_o (deg/hr/g)	0.5000007	0.5	0.0001
K_{ss} (deg/hr/g^2)	0.040064	0.04	0.16
K_{ii} (deg/hr/g^2)	-0.039625	-0.04	0.94
K_{si} (deg/hr/g^2)	0.020106	0.02	0.53
K_{io} (deg/hr/g^2)	0.0200658	0.02	0.33
K_{os} (deg/hr/g^2)	0.0202097	0.02	1.05

REFERENCES

1. Pitman, G. R., Jr., Editor, Inertial Guidance, New York: John-Wiley and Sons, Inc., 1962.

2. Russell, J. F., Gyroscope Standard Torque-to-Balance Test, Report MDC-TR-67-79, Holloman Air Force Base, New Mexico, June 1967.

3. Bonafede, W. J., "Tabe-Servo Gyro Evaluation," Section 6 of Notes for Summer 1963 Program 16.39S, Department of Aeronautics and Astronautics, MIT, Cambridge, Massachusetts, 1963.

4. Vaughn, R. S., "Test Methods for the Single Degree of Freedom Integrating Rate Gyro Phase II: Acceleration Sensitive Drift Characteristics," Report No. NADC-AI-6191, US Naval Air Development Center, Johnsville, Pennsylvania, December 1961.

5. Johnston, J. V., Analytical Solution for Two-Axis Tumble Test, Report No. RGL-73-11B, US Army Missile Research, Development and Engineering Laboratory, US Army Missile Command, Redstone Arsenal, Alabama, September 1973.

6. Lorenzini, D. A., "Testing of Precision Inertial Gyroscopes," AGARDograph No. 192, Advisory Group for Aerospace Research and Development, North Atlantic Treaty Organization, April 1973.

7. The Analytic Science Corporation, Reading, Massachusetts, "Dynamic Errors in Strapdown Inertial Navigation Systems," NASA CR-1962, 1971.

8. Oppenheim, A. V. and Schafer, R. W., Digital Signal Processing, Englewood Cliffs, New Jersey: Prentice-Hall, Inc., 1975.

9. Ralston, A., A First Course in Numerical Analysis, New York: McGraw-Hill Book Co., 1965.

10. Hung, J. C. and White, H. V., "Self-Alignment Techniques for Inertial Measurement Units," IEEE Transactions on Aerospace and Electronic Systems, Volume AES-11, No. 6, November 1975.

Appendix. ALGORITHM FOR OLD TWO-AXIS TUMBLE TEST

Let α and β be the incremental angular displacements of the table and gyro house, respectively, between two consecutive data taking points. Let $\phi = \theta = 0$ initially. Then at the k-th data taking point, $\phi = k\alpha$ and $\theta = k\beta$. Recalling the definition of D_4 and D_5 in Equation (16), then Equations (6), (7), and (8) can be expressed as

$$a_s(k) = D_4 \cos k\alpha \cos k\beta + D_5 \sin k\beta \qquad (52)$$

$$a_i(k) = -D_4 \sin k\alpha \qquad (53)$$

$$a_o(k) = D_4 \cos k\alpha \sin k\beta - D_5 \cos k\beta \quad . \qquad (54)$$

Define

$$b_{ss}(k) = a_s^2(k) \qquad (55)$$

$$b_{ii}(k) = a_i^2(k) \qquad (56)$$

$$b_{si}(k) = a_s(k) \, a_i(k) \qquad (57)$$

$$b_{io}(k) = a_i(k) \, a_o(k) \qquad (58)$$

$$b_{os}(k) = a_o(k) \, a_s(k) \quad . \qquad (59)$$

Substituting Equations (55) through (59) into Equation (4) gives

$$D(k) = D_o + K_s \, a_s(k) + K_i \, a_i(k) + K_o \, a_o(k)$$

$$+ K_{ss} \, b_{ss}(k) + K_{ii} \, b_{ii}(k)$$

$$+ K_{si} \, b_{si}(k) + K_{io} \, b_{io}(k) + K_{os} \, b_{os}(k) \quad . \qquad (60)$$

Using vector notation,

$$D(k) = \underline{C}^T(k)\, \underline{x} \tag{61}$$

where

$$\underline{C}(k) = \begin{bmatrix} 1 \\ a_s(k) \\ a_i(k) \\ a_o(k) \\ b_{ss}(k) \\ b_{ii}(k) \\ b_{si}(k) \\ b_{io}(k) \\ b_{os}(k) \end{bmatrix} \tag{62}$$

$$\underline{x} = \begin{bmatrix} D_o \\ K_s \\ K_i \\ K_o \\ K_{ss} \\ K_{ii} \\ K_{si} \\ K_{io} \\ K_{os} \end{bmatrix} \tag{63}$$

In Equation (61), $D(k)$ is the measured drift at the k-th time instant and $\underline{x}$ is the parameter vector to be determined. For a total of n measurements, there are n equations in the form of Equation (61). They can be arranged in a column as follows:

26

$$
\begin{bmatrix} D(1) \\ \vdots \\ D(k) \\ \vdots \\ D(n) \end{bmatrix} = \begin{bmatrix} \underline{c}^T(1) \\ \vdots \\ \underline{c}^T(k) \\ \vdots \\ \underline{c}^T(n) \end{bmatrix} \underline{x} \quad . \tag{64}
$$

$$\underbrace{\phantom{\begin{bmatrix} D(1) \end{bmatrix}}}_{\underline{z}} \quad \underbrace{\phantom{\begin{bmatrix} \underline{c}^T(1) \end{bmatrix}}}_{Q}$$

Define vector $\underline{z}$ and matrix Q as shown in Equation (64). In general, $n > 9$, so Q is not square and therefore cannot be inverted. An unique solution for $\underline{x}$ can be obtained using the pseudo inverse

$$\underline{x} = (Q^T Q)^{-1} Q^T \underline{z} \quad , \tag{65}$$

which is exactly the same as the least square regression formula used in Equations (45) and (48).

Equation (65) is a batch processing algorithm. It involves multiplication of $n \times 9$ matrices and inversion of a 9×9 matrix. The algorithm can be made sequential if so desired.

DISTRIBUTION

No. of Copies

Defense Documentation Center
Cameron Station
Alexandria, Virginia   22314   12

Commander
US Army Materiel Development and Readiness Command
ATTN: DRCRD   1
        DRCDL   1
5001 Eisenhower Avenue
Alexandria, Virginia   22333

DRSMI-FR, Mr. Strickland   1
     -LP, Mr. Voigt   1
     -R, Dr. McDaniel   1
         Dr. Kobler   1
     -RBD   3
     -RPR (Record Set)   1
         (Reference Copy)   1